Journal of Zhejiang University-SCIENCE C (Computers & Electronics)
ISSN 1869-1951 (Print); ISSN 1869-196X (Online)
www.zju.edu.cn/jzus; www.springerlink.com
E-mail: jzus@zju.edu.cn

Third harmonic distortion calculation of a self-oscillating power amplifier

Yu-hua CHENG, Nian-xiong TAN

(*Institute of VLSI Design, Zhejiang University, Hangzhou 310027, China*)

E-mail: {chengyh, ntan}@vlsi.zju.edu.cn

Received Apr. 15, 2010; Revision accepted Oct. 21, 2010; Crosschecked Jan. 31, 2011; Published online Mar. 4, 2011

Abstract: It is difficult to analyze the harmonic distortion of a self-oscillating power amplifier (SOPA), because the SOPA is a hard nonlinear system without an external clock. The single or multiple sinusoidal inputs describing function (DF) method is commonly used to linearize a nonlinear element, but this method considers only the components at the same frequencies as the input signals (i.e., fundamental components) at the nonlinear element's output. In this paper, besides the fundamental components, the third harmonic components are also calculated at the output of a comparator with three sinusoidal inputs, to create a linearized model of the comparator, and thus of the SOPA. The third harmonic distortion of the SOPA is calculated. The models of the zeroth and the first order SOPA are verified by behavioral simulation using MATLAB.

Key words: Describing function (DF), Comparator, Self-oscillating power amplifier (SOPA), Third harmonic distortion
doi:10.1631/jzus.C1000097 **Document code:** A **CLC number:** TN402

1 Introduction

A self-oscillating power amplifier (SOPA) is a closed-loop class-D amplifier without an external clock signal. SOPAs have been used in designing ADSL/VDSL (asymmetric digital subscriber line/ very-high-bit-rate digital subscriber line) line drivers (Piessens and Steyaert, 2001; 2003; 2005; de Gezelle *et al*., 2005; 2008; Serneels *et al*., 2007; Buyle *et al*., 2008) and audio power amplifiers (van der Hulst *et al*., 2002; Putzeys, 2005), due to their high efficiency. SOPAs have also been used as asynchronous sigma delta modulators to design analog-to-digital converters (Roza, 1997; Ouzounov *et al*., 2006; Daniels *et al*., 2008; 2010).

Fig. 1 shows the block diagram of the SOPA (Piessens and Steyaert, 2005). It consists of a comparator, a low-pass filter $F(s)$ in the forward path, and a low-pass filter $B(s)$ in the feedback path. $V_{\text{in,s}}$ and $V_{\text{out,s}}$ are the input and output signals, respectively.

The principle of the SOPA has been described in Piessens and Steyaert (2005). It is difficult to analyze the system behavior because of the hard nonlinear element, namely a comparator. The single or multiple sinusoidal inputs describing function (DF) method (Gelb and Velde, 1968) is commonly used to linearize the nonlinear element in the frequency domain when the input is a single or multiple sinusoid. Fig. 2 shows the linearization of a nonlinear element N using DFs. The input is the sum of $A_{\text{i},k}\sin(\omega_{\text{i},k}t+\theta_{\text{i},k})$ (k=1, 2, …, n), and the approximate output is the sum of $A_{\text{o},k}\sin(\omega_{\text{i},k}t+\theta_{\text{o},k})$ (k=1, 2, …, n) after linearization. The linearized model of N is a series of DFs. The DF of the signal $A_{\text{i},k}\sin(\omega_{\text{i},k}t+\theta_{\text{i},k})$ is G_k, which is defined as

$$G_k=\frac{A_{\text{o},k}}{A_{\text{i},k}}\angle(\theta_{\text{o},k}-\theta_{\text{i},k}),\quad k=1, 2, \ldots, n, \qquad (1)$$

where $A_{\text{o},k}/A_{\text{i},k}$ is the gain, and $\angle(\theta_{\text{o},k}-\theta_{\text{i},k})$ is the phase shift, which is the difference between $\theta_{\text{o},k}$ and $\theta_{\text{i},k}$. The sinusoidal input DF is aimed to obtain the amplitude and phase of the component at the same frequency as the input signal (i.e., the fundamental component) at the nonlinear element's output.

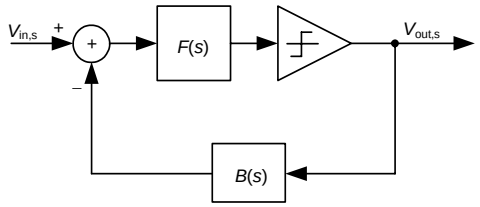

Fig. 1 Block diagram of the self-oscillating power amplifier (SOPA)

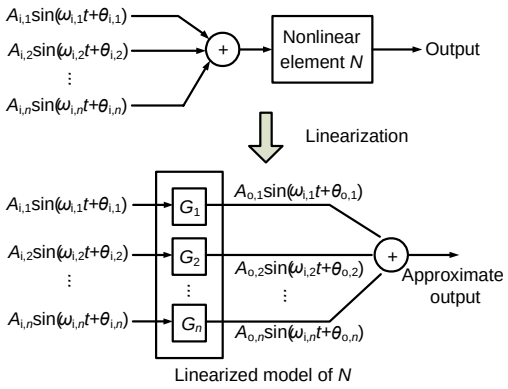

Fig. 2 Linearization of a nonlinear element using a describing function (DF)

In Piessens and Steyaert (2005), the input of the comparator of the SOPA was considered to have two sinusoidal inputs: $A_{\mathrm{osc}}\sin(\omega_{\mathrm{osc}}t+\theta_{\mathrm{osc}})$ at the oscillation frequency ω_{osc}, and $A_{\mathrm{in}}\sin(\omega_{\mathrm{in}}t+\theta_{\mathrm{in}})$ at the system's input frequency ω_{in}. The other signals were ignored due to their smaller amplitudes. The DF of the signal $A_{\mathrm{in}}\sin(\omega_{\mathrm{in}}t+\theta_{\mathrm{in}})$ was calculated using two sinusoidal inputs DF (Gelb and Velde, 1968; Piessens and Steyaert, 2005):

$$G(A_{\mathrm{in}}, A_{\mathrm{osc}}) = \frac{2V_{\mathrm{DD}}}{\pi A_{\mathrm{osc}}} + \frac{V_{\mathrm{DD}}}{4\pi A_{\mathrm{osc}}^3}A_{\mathrm{in}}^2 + \frac{3V_{\mathrm{DD}}}{32\pi A_{\mathrm{osc}}^5}A_{\mathrm{in}}^4 + \cdots, \tag{2}$$

where $\pm V_{\mathrm{DD}}$ are the high- and low-level outputs of the comparator, and A_{osc} and A_{in} are the amplitudes at frequencies ω_{osc} and ω_{in}, respectively. The signal at frequency ω_{in} at the comparator's output can be obtained, which is $A_{\omega_{\mathrm{in}}}\sin(\omega_{\mathrm{in}}t+\theta_{\mathrm{in}})$. The amplitude $A_{\omega_{\mathrm{in}}}$ is

$$\begin{aligned} A_{\omega_{\mathrm{in}}} &= G(A_{\mathrm{in}}, A_{\mathrm{osc}})A_{\mathrm{in}} \\ &= \frac{2V_{\mathrm{DD}}}{\pi A_{\mathrm{osc}}}A_{\mathrm{in}} + \frac{V_{\mathrm{DD}}}{4\pi A_{\mathrm{osc}}^3}A_{\mathrm{in}}^3 + \frac{3V_{\mathrm{DD}}}{32\pi A_{\mathrm{osc}}^5}A_{\mathrm{in}}^5 + \cdots. \end{aligned} \tag{3}$$

However, the sinusoidal input DF describes only the component at the fundamental frequency ω_{in}, and cannot deal with the harmonic components. Piessens and Steyaert (2005) took the second term in Eq. (3) as the source of the third harmonic component produced by the comparator. After substituting $A_{\mathrm{in}}\sin(\omega_{\mathrm{in}}t+\theta_{\mathrm{in}})$ for A_{in} in Eq. (3) and using the trigonometric function formula $\sin^3 x = 3\sin x/4 - \sin(3x)/4$, the third harmonic component is obtained.

The estimation has good accuracy, but the disadvantage that replacing the amplitude A_{in} with the signal $A_{\mathrm{in}}\sin(\omega_{\mathrm{in}}t+\theta_{\mathrm{in}})$ is not strict. In fact, the third harmonic component can be calculated using the same method as the fundamental component calculation in DF calculation, which will be stated in detail in Section 2.

As the SOPA is a closed-loop system, in order to calculate its third harmonic distortion, the loop gain at frequency $3\omega_{\mathrm{in}}$ should be known. In the loop, the comparator's gain of the signal at frequency $3\omega_{\mathrm{in}}$ should be calculated using the three sinusoidal inputs DF (Piessens and Steyaert, 2005). The three sinusoid frequencies are ω_{osc}, ω_{in}, and $3\omega_{\mathrm{in}}$. The gain at $3\omega_{\mathrm{in}}$ is estimated as a quarter of the comparator's gain when only $A_{\mathrm{osc}}\sin(\omega_{\mathrm{osc}}t+\theta_{\mathrm{osc}})$ exists at the input of the comparator (Piessens and Steyaert, 2005). In this work, the mathematical derivation of the comparator's gain at $3\omega_{\mathrm{in}}$ is given using three sinusoidal inputs DF.

2 Comparator's linearized model with three sinusoidal inputs

The comparator and the relationship between its input and output are shown in Fig. 3, where the input is x, and the output is $y(x)$, and $\pm V_{\mathrm{DD}}$ are the high- and low-level outputs of the comparator.

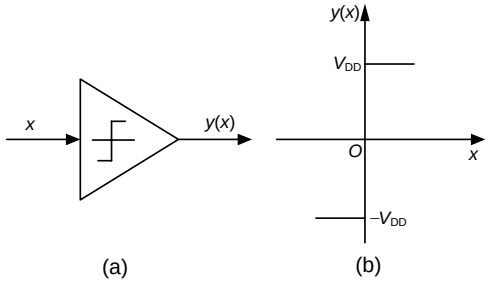

Fig. 3 The comparator (a) and the relationship between its input and output (b)

The output $y(x)$ is given by

$$y(x)=\begin{cases}V_{\mathrm{DD}}, & \text{for } x\geq 0,\\ -V_{\mathrm{DD}}, & \text{for } x<0.\end{cases} \tag{4}$$

The Fourier transform and the inverse Fourier transform are

$$Y(\mathrm{j}\omega)=\int_{-\infty}^{\infty}y(x)\mathrm{e}^{-\mathrm{j}\omega x}\mathrm{d}x, \tag{5}$$

$$y(x)=\frac{1}{2\pi}\int_{-\infty}^{\infty}Y(\mathrm{j}\omega)\mathrm{e}^{\mathrm{j}\omega x}\mathrm{d}\omega. \tag{6}$$

In a SOPA, the comparator's input can be considered as the sum of three sinusoids at frequencies ω_{osc}, ω_{in}, and $3\omega_{\mathrm{in}}$, with amplitudes A_{osc}, A_{in}, and $A_{3\mathrm{in}}$, respectively, and initial phases θ_{osc}, θ_{in}, and $\theta_{3\mathrm{in}}$, respectively:

$$\begin{aligned}x=&A_{\mathrm{osc}}\sin(\omega_{\mathrm{osc}}t+\theta_{\mathrm{osc}})+A_{\mathrm{in}}\sin(\omega_{\mathrm{in}}t+\theta_{\mathrm{in}})\\&+A_{3\mathrm{in}}\sin(\omega_{3\mathrm{in}}t+\theta_{3\mathrm{in}}),\end{aligned} \tag{7}$$

where $\omega_{3\mathrm{in}}=3\omega_{\mathrm{in}}$. Usually the conditions $A_{\mathrm{osc}}>A_{\mathrm{in}}>>A_{3\mathrm{in}}$ and $\omega_{\mathrm{osc}}>>\omega_{3\mathrm{in}}$ are always satisfied in a SOPA, since a linear modulation is wanted (Piessens and Steyaert, 2005). If $\varphi_{\mathrm{osc}}=\omega_{\mathrm{osc}}t+\theta_{\mathrm{osc}}$, $\varphi_{\mathrm{in}}=\omega_{\mathrm{in}}t+\theta_{\mathrm{in}}$, and $\varphi_{3\mathrm{in}}=\omega_{3\mathrm{in}}t+\theta_{3\mathrm{in}}$ are noted, substituting Eq. (7) into Eq. (6) results in

$$\begin{aligned}y=\frac{1}{2\pi}\int_{-\infty}^{\infty}\big(&Y(\mathrm{j}\omega)\exp(\mathrm{j}\omega A_{\mathrm{osc}}\sin\varphi_{\mathrm{osc}}\\&+\mathrm{j}\omega A_{\mathrm{in}}\sin\varphi_{\mathrm{in}}+\mathrm{j}\omega A_{3\mathrm{in}}\sin\varphi_{3\mathrm{in}})\big)\mathrm{d}\omega.\end{aligned} \tag{8}$$

The exponentials can be expanded using the following equation:

$$\begin{aligned}\mathrm{e}^{\mathrm{j}z\sin\theta}=&\sum_{n=0}^{\infty}\varepsilon_n J_{2n}(z)\cos(2n\theta)\\&+2\mathrm{j}\sum_{n=0}^{\infty}J_{2n+1}(z)\sin\big((2n+1)\theta\big),\end{aligned} \tag{9}$$

$$\varepsilon_n=\begin{cases}1, & \text{for } n=0,\\ 2, & \text{for } n=1,\ 2,\ 3,\ \cdots,\end{cases}$$

where $J_n(z)$ is the first kind Bessel function of order n and argument z (Abramowitz and Stegun, 1972).

Then the integrand in Eq. (8) becomes a series multiplied by $Y(\mathrm{j}\omega)$ as shown in Eq. (10):

$$\begin{aligned}&Y(\mathrm{j}\omega)\exp\big(\mathrm{j}\omega(A_{\mathrm{osc}}\sin\varphi_{\mathrm{osc}}+A_{\mathrm{in}}\sin\varphi_{\mathrm{in}}+A_{3\mathrm{in}}\sin\varphi_{3\mathrm{in}})\big)\\&=Y(\mathrm{j}\omega)\cdot\Bigg(\sum_{m=0}^{\infty}\varepsilon_m J_{2m}(A_{\mathrm{osc}})\cos(2m\varphi_{\mathrm{osc}})\\&\qquad+2\mathrm{j}\sum_{m=0}^{\infty}J_{2m+1}(A_{\mathrm{osc}})\sin\big((2m+1)\varphi_{\mathrm{osc}}\big)\Bigg)\\&\quad\cdot\Bigg(\sum_{n=0}^{\infty}\varepsilon_n J_{2n}(A_{\mathrm{in}})\cos(2n\varphi_{\mathrm{in}})\\&\qquad+2\mathrm{j}\sum_{n=0}^{\infty}J_{2n+1}(A_{\mathrm{in}})\sin\big((2n+1)\varphi_{\mathrm{in}}\big)\Bigg)\\&\quad\cdot\Bigg(\sum_{p=0}^{\infty}\varepsilon_p J_{2p}(A_{3\mathrm{in}})\cos(2p\varphi_{3\mathrm{in}})\\&\qquad+2\mathrm{j}\sum_{p=0}^{\infty}J_{2p+1}(A_{3\mathrm{in}})\sin\big((2p+1)\varphi_{3\mathrm{in}}\big)\Bigg).\end{aligned} \tag{10}$$

If the integrand is an odd function of the integral variable, the value of the integral of this integrand over the doubly infinite range is zero. For the ideal comparator, we have $Y(\mathrm{j}\omega)=2V_{\mathrm{DD}}/(\mathrm{j}\omega)$ (Piessens and Steyaert, 2005), which is an odd function of ω. Based on the fact that Bessel functions of odd orders are odd and those of even orders are even, Eq. (8) can be simplified as

$$y=y_1+y_2+y_3+y_4, \tag{11}$$

$$\begin{aligned}&y_1=4V_{\mathrm{DD}}/\pi\\&\cdot\sum_{m=0}^{\infty}\sum_{n=0}^{\infty}\sum_{p=0}^{\infty}\Bigg(\int_0^{\infty}\frac{1}{\omega}J_{2m}(A_{\mathrm{osc}}\omega)J_{2n}(A_{\mathrm{in}}\omega)J_{2p+1}(A_{3\mathrm{in}}\omega)\mathrm{d}\omega\\&\quad\cdot\varepsilon_m\varepsilon_n\cos(2m\varphi_{\mathrm{osc}})\cos(2n\varphi_{\mathrm{in}})\sin\big((2p+1)\varphi_{3\mathrm{in}}\big)\Bigg),\end{aligned} \tag{12}$$

$$\begin{aligned}&y_2=4V_{\mathrm{DD}}/\pi\\&\cdot\sum_{m=0}^{\infty}\sum_{n=0}^{\infty}\sum_{p=0}^{\infty}\Bigg(\int_0^{\infty}\frac{1}{\omega}J_{2m}(A_{\mathrm{osc}}\omega)J_{2n+1}(A_{\mathrm{in}}\omega)J_{2p}(A_{3\mathrm{in}}\omega)\mathrm{d}\omega\\&\quad\cdot\varepsilon_m\varepsilon_p\cos(2m\varphi_{\mathrm{osc}})\sin\big((2n+1)\varphi_{\mathrm{in}}\big)\cos(2p\varphi_{3\mathrm{in}})\Bigg),\end{aligned} \tag{13}$$

$$\begin{aligned}&y_3=4V_{\mathrm{DD}}/\pi\\&\cdot\sum_{m=0}^{\infty}\sum_{n=0}^{\infty}\sum_{p=0}^{\infty}\Bigg(\int_0^{\infty}\frac{1}{\omega}J_{2m+1}(A_{\mathrm{osc}}\omega)J_{2n}(A_{\mathrm{in}}\omega)J_{2p}(A_{3\mathrm{in}}\omega)\mathrm{d}\omega\\&\quad\cdot\varepsilon_n\varepsilon_p\sin\big((2m+1)\varphi_{\mathrm{osc}}\big)\cos(2n\varphi_{\mathrm{in}})\cos(2p\varphi_{3\mathrm{in}})\Bigg),\end{aligned} \tag{14}$$

$$y_4=-16V_{\mathrm{DD}}/\pi \cdot\sum_{m=0}^{\infty}\sum_{n=0}^{\infty}\sum_{p=0}^{\infty}\left(\int_0^{\infty}\frac{1}{\omega}J_{2m+1}(A_{\mathrm{osc}}\omega)J_{2n+1}(A_{\mathrm{in}}\omega)J_{2p+1}(A_{3\mathrm{in}}\omega)\mathrm{d}\omega \cdot\sin\big((2m+1)\varphi_{\mathrm{osc}}\big)\sin\big((2n+1)\varphi_{\mathrm{in}}\big)\sin\big((2p+1)\varphi_{3\mathrm{in}}\big)\right). \tag{15}$$

It can be observed that all the integrands in Eqs. (12)–(15) are even functions of ω.

The different combinations of m, n, and p result in different frequency components. The key is to solve the infinite integral of the product of three Bessel functions. For arbitrary m, n, and p in Eqs. (12)–(15), the integrals cannot be solved (Ekstrom, 1960). Eq. (16) gives the conditions upon which the integral can be solved (Bailey, 1936):

$$\int_0^{\infty}\frac{1}{\omega}J_{\mu}(A_{3\mathrm{in}}\omega)J_{\nu}(A_{\mathrm{in}}\omega)J_{\rho}(A_{\mathrm{osc}}\omega)\mathrm{d}\omega =\frac{A_{3\mathrm{in}}^{\mu}A_{\mathrm{in}}^{\nu}\Gamma\left(\frac{\mu+\nu+\rho}{2}\right)}{2A_{\mathrm{osc}}^{\mu+\nu}\Gamma(\mu+1)\Gamma(\nu+1)\Gamma\left(1-\frac{\mu+\nu-\rho}{2}\right)} \cdot F_4\left(\frac{\mu+\nu-\rho}{2},\frac{\mu+\nu+\rho}{2};\mu+1,\nu+1;\left(\frac{A_{3\mathrm{in}}}{A_{\mathrm{osc}}}\right)^2,\left(\frac{A_{\mathrm{in}}}{A_{\mathrm{osc}}}\right)^2\right),$$
$$\text{for } \mu+\nu>\rho\geq 0,\ A_{\mathrm{osc}}>A_{\mathrm{in}}+A_{3\mathrm{in}},\ A_{\mathrm{in}}>0,\ A_{3\mathrm{in}}>0. \tag{16}$$

Herein, μ, ν, and ρ are the orders of the three Bessel functions, respectively; A_{osc}, A_{in}, and $A_{3\mathrm{in}}$ are the amplitudes of the three input signals, respectively; $F_4(a,b;c,d;x,y)$ is the Appell hyper-geometric function with arguments a, b, c, d, x, and y, which can be expanded as (Bailey, 1936)

$$F_4(a,b;c,d;x,y)=\sum_{r=0}^{\infty}\sum_{s=0}^{\infty}\frac{(a)_{r+s}(b)_{r+s}}{(c)_r(d)_s r!s!}x^r y^s, \tag{17}$$

$$(z)_n=\Gamma(z+n)/\Gamma(z), \tag{18}$$

where r and s are non-negative integers, $(z)_n$ is the Pochhammer symbol of arguments z and n, and $\Gamma(z)$ is the Gamma function of argument z (Abramowitz and Stegun, 1972).

All the possible components of the output signal at the different frequencies can be seen in Eqs. (12)–(15). The fundamental, harmonic, and intermodulation components may be superimposed. Here, only the components at ω_{in} and $3\omega_{\mathrm{in}}$ are concerned.

All the combinations of μ, ν, and ρ that satisfy $|\rho\omega_{\mathrm{osc}}\pm\mu\omega_{3\mathrm{in}}\pm\nu\omega_{\mathrm{in}}|=3\omega_{\mathrm{in}}$ contribute to the component at $3\omega_{\mathrm{in}}$ (μ, ν, and ρ are non-negative integers).

The order of the harmonic or intermodulation is defined by the value $\mu+\nu+\rho$. In general, the amplitudes of the harmonic or intermodulation components decrease with the increase of the order. Thus, only the components with low orders need to be considered. Because $\omega_{\mathrm{osc}}>>\omega_{\mathrm{in}}$ and $\omega_{\mathrm{osc}}>>\omega_{3\mathrm{in}}$, ρ should be 0; otherwise, the order $\mu+\nu+\rho$ should be large to satisfy $|\rho\omega_{\mathrm{osc}}\pm\mu\omega_{3\mathrm{in}}\pm\nu\omega_{\mathrm{in}}|=3\omega_{\mathrm{in}}$. When $\rho=0$, $\omega_{3\mathrm{in}}=3\omega_{\mathrm{in}}$ results in $\nu=3\mu+3$ (μ is a non-negative integer) or $\nu=3\mu-3$ (μ is a positive integer). The two lowest order components cases are $\rho=0$, $\mu=0$, $\nu=3$ and $\rho=0$, $\mu=1$, $\nu=0$.

By choosing $m=0$, $n=1$, $p=0$ in Eq. (13), the third harmonic component produced by the signal $A_{\mathrm{in}}\sin(\omega_{\mathrm{in}}t+\theta_{\mathrm{in}})$ can be obtained. It is $A_{3\omega_{\mathrm{in}}}\sin(3\omega_{\mathrm{in}}t+3\theta_{\mathrm{in}}+\pi)$, where the amplitude is calculated as

$$\begin{aligned}A_{3\omega_{\mathrm{in}}}&=\left|\frac{4V_{\mathrm{DD}}}{\pi}\int_0^{\infty}\frac{1}{\omega}J_0(A_{3\mathrm{in}}\omega)J_3(A_{\mathrm{in}}\omega)J_0(A_{\mathrm{osc}}\omega)\mathrm{d}\omega\right|\\&=\left|-\frac{V_{\mathrm{DD}}}{12\pi}\left(\frac{A_{\mathrm{in}}}{A_{\mathrm{osc}}}\right)^3\sum_{r=0}^{\infty}\sum_{s=0}^{\infty}\frac{(1.5)_{r+s}(1.5)_{r+s}}{(1)_r(4)_s r!s!}\left(\frac{A_{3\mathrm{in}}}{A_{\mathrm{osc}}}\right)^{2r}\left(\frac{A_{\mathrm{in}}}{A_{\mathrm{osc}}}\right)^{2s}\right|\\&=\frac{V_{\mathrm{DD}}}{12\pi}\left(\frac{A_{\mathrm{in}}}{A_{\mathrm{osc}}}\right)^3\left(1+\frac{9}{16}\left(\frac{A_{\mathrm{in}}}{A_{\mathrm{osc}}}\right)^2+\frac{9}{4}\left(\frac{A_{3\mathrm{in}}}{A_{\mathrm{osc}}}\right)^2+\frac{225}{64}\left(\frac{A_{3\mathrm{in}}}{A_{\mathrm{osc}}}\right)^2\left(\frac{A_{\mathrm{in}}}{A_{\mathrm{osc}}}\right)^2+\cdots\right),\end{aligned} \tag{19}$$

and the initial phase is shifted from θ_{in} to $3\theta_{\mathrm{in}}+\pi$ according to Eqs. (13) and (19). By choosing $m=0$, $n=0$, $p=0$ in Eq. (12), the fundamental component produced by signal $A_{3\mathrm{in}}\sin(\omega_{3\mathrm{in}}t+\theta_{3\mathrm{in}})$ can be obtained. It is $A_{\omega_{3\mathrm{in}}}\sin(\omega_{3\mathrm{in}}t+\theta_{3\mathrm{in}})$, where the amplitude is calculated as

$$\begin{aligned}A_{\omega_{3\mathrm{in}}}&=\left|\frac{4V_{\mathrm{DD}}}{\pi}\int_0^{\infty}\frac{1}{\omega}J_1(A_{3\mathrm{in}}\omega)J_0(A_{\mathrm{in}}\omega)J_0(A_{\mathrm{osc}}\omega)\mathrm{d}\omega\right|\\&=\left|\frac{2V_{\mathrm{DD}}}{\pi}\frac{A_{3\mathrm{in}}}{A_{\mathrm{osc}}}\sum_{r=0}^{\infty}\sum_{s=0}^{\infty}\frac{(0.5)_{r+s}(0.5)_{r+s}}{(2)_r(1)_s r!s!}\left(\frac{A_{3\mathrm{in}}}{A_{\mathrm{osc}}}\right)^{2r}\left(\frac{A_{\mathrm{in}}}{A_{\mathrm{osc}}}\right)^{2s}\right|\\&=\frac{2V_{\mathrm{DD}}}{\pi}\frac{A_{3\mathrm{in}}}{A_{\mathrm{osc}}}\left(1+\frac{1}{8}\left(\frac{A_{3\mathrm{in}}}{A_{\mathrm{osc}}}\right)^2+\frac{1}{4}\left(\frac{A_{\mathrm{in}}}{A_{\mathrm{osc}}}\right)^2+\frac{9}{32}\left(\frac{A_{3\mathrm{in}}}{A_{\mathrm{osc}}}\right)^2\left(\frac{A_{\mathrm{in}}}{A_{\mathrm{osc}}}\right)^2+\cdots\right),\end{aligned} \tag{20}$$

and the initial phase is not shifted according to Eqs. (12) and (20).

Similarly, all the combinations of μ, v, and ρ that satisfy $|\rho\omega_{osc}\pm\mu\omega_{3in}\pm v\omega_{in}|=\omega_{in}$ contribute to the component at ω_{in} (μ, v, and ρ are non-negative integers). The lowest order component case is $\rho=0$, $\mu=0$, $v=1$. By choosing $m=0$, $n=0$, $p=0$ in Eq. (13), the fundamental component produced by the signal $A_{in}\sin(\omega_{in}t+\theta_{in})$ can be obtained. It is $A_{\omega_{in}}\sin(\omega_{in}t+\theta_{in})$, where the amplitude is calculated as

$$\begin{aligned}A_{\omega_{in}}&=\left|\frac{4V_{DD}}{\pi}\int_0^{\infty}\frac{1}{\omega}J_0(A_{3in}\omega)J_1(A_{in}\omega)J_0(A_{osc}\omega)\mathrm{d}\omega\right|\\&=\left|\frac{2V_{DD}}{\pi}\frac{A_{in}}{A_{osc}}\sum_{r=0}^{\infty}\sum_{s=0}^{\infty}\frac{(0.5)_{r+s}(0.5)_{r+s}}{(1)_r(2)_s r!s!}\left(\frac{A_{3in}}{A_{osc}}\right)^{2r}\left(\frac{A_{in}}{A_{osc}}\right)^{2s}\right|\\&=\frac{2V_{DD}}{\pi}\frac{A_{in}}{A_{osc}}\left(1+\frac{1}{8}\left(\frac{A_{in}}{A_{osc}}\right)^2+\frac{1}{4}\left(\frac{A_{3in}}{A_{osc}}\right)^2\right.\\&\quad\left.+\frac{9}{32}\left(\frac{A_{in}}{A_{osc}}\right)^2\left(\frac{A_{3in}}{A_{osc}}\right)^2+\cdots\right),\end{aligned}\tag{21}$$

and the initial phase is not shifted according to Eqs. (13) and (21).

Similarly, all the combinations of μ, v, and ρ that satisfy $|\rho\omega_{osc}\pm\mu\omega_{3in}\pm v\omega_{in}|=\omega_{osc}$ contribute to the component at ω_{osc} (μ, v, and ρ are non-negative integers). In case of the lowest order, i.e., $\rho=1$, $\mu=0$, $v=0$, the integral in Eq. (16) cannot be solved because the condition $\mu+v>\rho\geq 0$ cannot be satisfied. However, the sinusoid $A_{osc}\sin(\omega_{osc}t+\theta_{osc})$ dominates in the comparator's input as $A_{osc}>A_{in}>>A_{3in}$. If we ignore the other signals due to their much smaller amplitudes, the amplitude at ω_{osc} at the comparator's output can be solved using the single sinusoidal input DF (Piessens and Steyaert, 2005):

$$A_{\omega_{osc}}=4V_{DD}/\pi.\tag{22}$$

The DFs of the signals $A_{3in}\sin(\omega_{3in}t+\theta_{3in})$, $A_{in}\sin(\omega_{in}t+\theta_{in})$, and $A_{osc}\sin(\omega_{osc}t+\theta_{osc})$ are derived from Eqs. (20), (21), and (22), respectively, and are given as follows:

$$\begin{aligned}G_{3in}&=\frac{2V_{DD}}{\pi A_{osc}}\left(1+\frac{1}{8}\left(\frac{A_{3in}}{A_{osc}}\right)^2+\frac{1}{4}\left(\frac{A_{in}}{A_{osc}}\right)^2\right.\\&\quad\left.+\frac{9}{32}\left(\frac{A_{3in}}{A_{osc}}\right)^2\left(\frac{A_{in}}{A_{osc}}\right)^2+\cdots\right)\approx\frac{2V_{DD}}{\pi A_{osc}},\end{aligned}\tag{23}$$

$$\begin{aligned}G_{in}&=\frac{2V_{DD}}{\pi A_{osc}}\left(1+\frac{1}{8}\left(\frac{A_{in}}{A_{osc}}\right)^2+\frac{1}{4}\left(\frac{A_{3in}}{A_{osc}}\right)^2\right.\\&\quad\left.+\frac{9}{32}\left(\frac{A_{in}}{A_{osc}}\right)^2\left(\frac{A_{3in}}{A_{osc}}\right)^2+\cdots\right)\approx\frac{2V_{DD}}{\pi A_{osc}},\end{aligned}\tag{24}$$

$$G_{osc}=\frac{4V_{DD}}{\pi A_{osc}}.\tag{25}$$

The three DFs do not have the phase shift. As observed from Eqs. (23) and (24), the two gains are almost equal, and both can be denoted as G, approximately equal to $0.5G_{osc}$. The comparator's linearized model at ω_{in} and ω_{3in} is shown in Fig. 4. The additive term at the comparator's output at $3\omega_{in}$ is given by Eq. (19). It can be stated that the large amplitude signal $A_{osc}\sin(\omega_{osc}t+\theta_{osc})$ linearizes the comparator for the other signals; i.e., the other signals' gain, G, is not the function of themselves.

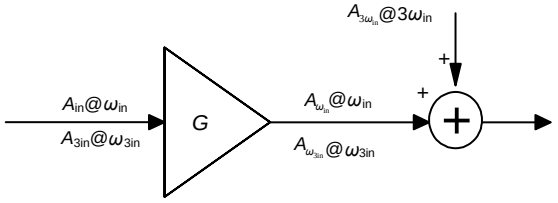

Fig. 4 Comparator's linearized model at ω_{in} and ω_{3in}

There are two differences between this linearized model derived in this work and the one in Piessens and Steyaert (2005). The additive term $A_{3\omega_{in}}$ is $V_{DD}/(16\pi)\cdot(A_{in}/A_{osc})^3$ and the comparator's gain at $3\omega_{in}$ is $V_{DD}/(\pi A_{osc})=0.25G_{osc}$ in Piessens and Steyaert (2005).

3 Simulation of the comparator's linearized model

Fig. 5 shows the simulation and calculation results of the amplitudes at $3\omega_{in}$ relative to A_{in} at the comparator's output, as a function of A_{in}/V_{DD}. The three sinusoidal inputs are $A_{osc}\sin(\omega_{osc}t+\theta_{osc})$, $A_{in}\sin(\omega_{in}t+\theta_{in})$, and $A_{3in}\sin(\omega_{3in}t+\theta_{3in})$, where $A_{osc}=1$ V, $\omega_{osc}=34.6\pi$ Mrad/s, $\theta_{osc}=0$ rad, $\omega_{in}=2\pi$ Mrad/s, $\theta_{in}=\pi$ rad, $A_{3in}=0.001$ V, $\omega_{3in}=6\pi$ Mrad/s, $\theta_{3in}=0$ rad. The comparator's high- and low-level outputs are $\pm V_{DD}=\pm 1$ V. The simulation environment is

MATLAB SIMULINK with an ODE45 solver. The amplitudes of the simulation results are derived from a 10^7-point discrete Fourier transform (DFT) of the comparator's output with a simulation time of 10 μs and a sampling time of 1 ps. The window function of the DFT is Hanning. For the calculation, the first 50 terms of Eqs. (19) and (20) are used, and the signal at $3\omega_{in}$ at the comparator's output is $A_{3\omega_{in}}\sin(3\omega_{in}t+3\theta_{in}+\pi)+A_{\omega_{3in}}\sin(\omega_{3in}t+\theta_{3in})$, as described in Section 2. The amplitude of this signal, A_{sum}, is shown in Eq. (26), which also shows the impact of the initial phases. In this example, $3\theta_{in}+\pi-\theta_{3in}=4\pi$, so $A_{sum}=A_{3\omega_{in}}+A_{\omega_{3in}}$.

$$A_{sum}=\sqrt{A_{3\omega_{in}}^2+A_{\omega_{3in}}^2+2A_{3\omega_{in}}A_{\omega_{3in}}\cos(3\theta_{in}+\pi-\theta_{3in})}. \tag{26}$$

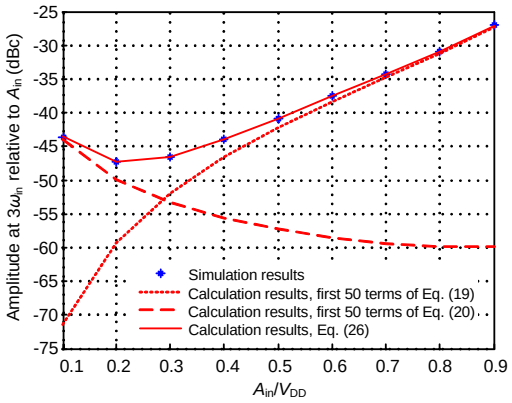

Fig. 5 Amplitudes at frequency $3\omega_{in}$ relative to A_{in} as a function of A_{in}/V_{DD}

The simulation results are consistent with the calculation results. When A_{in} is small (for example, smaller than $0.1V_{DD}$), the dominant component is $A_{\omega_{3in}}$; when A_{in} is large (for example, larger than $0.5V_{DD}$), the dominant component is $A_{3\omega_{in}}$.

Eqs. (19) and (20) can be simplified to reduce the calculation work, as will be used in the following section. The first two terms of Eq. (19) and the first term of Eq. (20) are calculated. Fig. 6 shows that the simplified equations results also agree with the simulation results with small errors.

4 Calculation of the SOPA's third harmonic distortion

The block diagram of the SOPA is as shown in Fig. 1. The oscillation with a zero input is called the

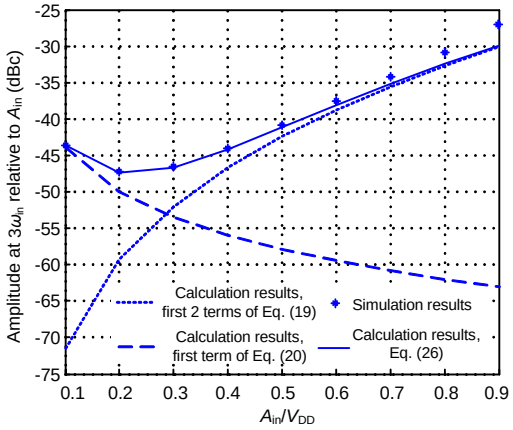

Fig. 6 Amplitudes at frequency $3\omega_{in}$ relative to A_{in} as a function of A_{in}/V_{DD} using simplified equations

limit cycle oscillation, and the oscillation frequency is called the limit cycle frequency, noted as ω_{LC}. In the limit cycle oscillation, the gain of the comparator G_{LC} is the same as the gain given by Eq. (25), with A_{osc} being A_{LC}. A_{LC} is the amplitude at ω_{LC} at the input of the comparator in the limit cycle oscillation case.

According to the Barkhausen criterion, we can derive (Piessens and Steyaert, 2005)

$$G_{LC}=1/\left|F(j\omega_{LC})B(j\omega_{LC})\right|, \tag{27}$$

$$A_{LC}=2V_{DD}\left|F(j\omega_{LC})B(j\omega_{LC})\right|/\pi, \tag{28}$$

where $F(j\omega_{LC})$ and $B(j\omega_{LC})$ are the values of $F(s)$ and $B(s)$ with $s=j\omega_{LC}$, respectively. The limit cycle oscillation frequency ω_{LC} is determined by the transfer function of the filters.

When the sinusoidal input $V_{in,s}=A_{in,s}\sin(\omega_{in}t)$ is applied to the system, the forced oscillation frequency, ω_{osc}, and the amplitude at ω_{osc} at the input of the comparator, A_{osc}, depend on the input signal (Piessens and Steyaert, 2005). But ω_{osc} and A_{osc} can be, however, approximately equal to ω_{LC} and A_{LC}, respectively, especially when the system sinusoidal input's amplitude $A_{in,s}$ is relatively small compared with V_{DD} (Piessens and Steyaert, 2005). This approximation is valid as long as $A_{in,s}$ is sufficiently small. In the desired working region of the SOPA, this condition is always fulfilled, because a linear modulation is desired (Piessens and Steyaert, 2005). Thus, the comparator's gain at ω_{osc}, G_{osc}, is approximately equal to G_{LC}.

According to Eqs. (23)–(25) and (27), the comparator's gain at ω_{in} and $3\omega_{in}$, G, is

$$G \approx \frac{G_{\mathrm{LC}}}{2} = \frac{1}{2\left|F(\mathrm{j}\omega_{\mathrm{osc}})B(\mathrm{j}\omega_{\mathrm{osc}})\right|}, \tag{29}$$

where $F(\mathrm{j}\omega_{\mathrm{osc}})$ and $B(\mathrm{j}\omega_{\mathrm{osc}})$ are the values of $F(s)$ and $B(s)$ with $s=\mathrm{j}\omega_{\mathrm{osc}}$, respectively. It can be observed that the gain G depends on the filters.

By replacing the comparator in Fig. 1 with its linearized model, the linearized mode of the SOPA can be derived (Fig. 7). $A_{\mathrm{in,s}}$, A_{in}, and $A_{\mathrm{out,s}}$ are the amplitudes of the system input signal, the comparator input signal, and the system output signal at frequency ω_{in}, respectively; $A_{3\mathrm{in}}$, $A_{3\omega_{\mathrm{in}}}$, and HD_3 are the amplitude of the comparator input signal, the amplitude of the additive signal at the comparator's output, and the third harmonic distortion at frequency $3\omega_{\mathrm{in}}$, respectively.

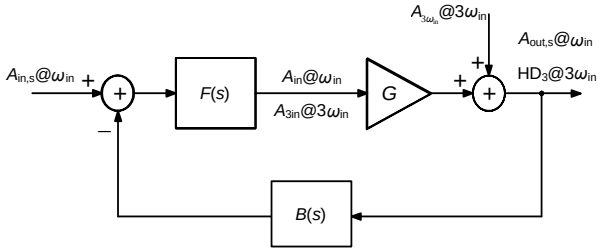

Fig. 7 Linearized model of the self-oscillating power amplifier (SOPA)

The open-loop gain $\mathrm{LG}_{\mathrm{in}}$ at ω_{in}, and the amplitudes $A_{\mathrm{out,s}}$ and A_{in} can be derived from Fig. 7:

$$\mathrm{LG}_{\mathrm{in}} = \left|F(\mathrm{j}\omega_{\mathrm{in}})B(\mathrm{j}\omega_{\mathrm{in}})G\right| = \left|\frac{F(\mathrm{j}\omega_{\mathrm{in}})B(\mathrm{j}\omega_{\mathrm{in}})}{2F(\mathrm{j}\omega_{\mathrm{osc}})B(\mathrm{j}\omega_{\mathrm{osc}})}\right|, \tag{30}$$

$$\begin{aligned} A_{\mathrm{out,s}} &= \left|\frac{F(\mathrm{j}\omega_{\mathrm{in}})G}{1+F(\mathrm{j}\omega_{\mathrm{in}})B(\mathrm{j}\omega_{\mathrm{in}})G}\right| A_{\mathrm{in,s}} \\ &= \left|\frac{F(\mathrm{j}\omega_{\mathrm{in}})}{2\left|F(\mathrm{j}\omega_{\mathrm{osc}})B(\mathrm{j}\omega_{\mathrm{osc}})\right| + F(\mathrm{j}\omega_{\mathrm{in}})B(\mathrm{j}\omega_{\mathrm{in}})}\right| A_{\mathrm{in,s}}, \end{aligned} \tag{31}$$

$$\begin{aligned} A_{\mathrm{in}} &= \left|\frac{F(\mathrm{j}\omega_{\mathrm{in}})}{1+F(\mathrm{j}\omega_{\mathrm{in}})B(\mathrm{j}\omega_{\mathrm{in}})G}\right| A_{\mathrm{in,s}} \\ &= \left|\frac{2F(\mathrm{j}\omega_{\mathrm{osc}})B(\mathrm{j}\omega_{\mathrm{osc}})F(\mathrm{j}\omega_{\mathrm{in}})}{2\left|F(\mathrm{j}\omega_{\mathrm{osc}})B(\mathrm{j}\omega_{\mathrm{osc}})\right| + F(\mathrm{j}\omega_{\mathrm{in}})B(\mathrm{j}\omega_{\mathrm{in}})}\right| A_{\mathrm{in,s}}, \end{aligned} \tag{32}$$

where $F(\mathrm{j}\omega_{\mathrm{in}})$ and $B(\mathrm{j}\omega_{\mathrm{in}})$ are the values of $F(s)$ and $B(s)$ with $s=\mathrm{j}\omega_{\mathrm{in}}$, respectively.

The amplitude $A_{3\mathrm{in}}$ and the third harmonic distortion HD_3 can be derived from Eqs. (19), (29), (32), and Fig. 7:

$$\begin{aligned} A_{3\mathrm{in}} &= \left|\frac{F(\mathrm{j}3\omega_{\mathrm{in}})B(\mathrm{j}3\omega_{\mathrm{in}})}{1+F(\mathrm{j}3\omega_{\mathrm{in}})B(\mathrm{j}3\omega_{\mathrm{in}})G}\right| A_{3\omega_{\mathrm{in}}} \\ &= \left|\frac{F(\mathrm{j}3\omega_{\mathrm{in}})B(\mathrm{j}3\omega_{\mathrm{in}})}{1+F(\mathrm{j}3\omega_{\mathrm{in}})B(\mathrm{j}3\omega_{\mathrm{in}})G}\right| \frac{V_{\mathrm{DD}}}{24\pi}\left(\frac{A_{\mathrm{in}}}{A_{\mathrm{osc}}}\right)^3 \left(1+\frac{9}{16}\left(\frac{A_{\mathrm{in}}}{A_{\mathrm{osc}}}\right)^2\right) \\ &= \frac{V_{\mathrm{DD}}}{12\pi}\cdot\left|\frac{F(\mathrm{j}\omega_{\mathrm{osc}})B(\mathrm{j}\omega_{\mathrm{osc}})F(\mathrm{j}3\omega_{\mathrm{in}})B(\mathrm{j}3\omega_{\mathrm{in}})}{2\left|F(\mathrm{j}\omega_{\mathrm{osc}})B(\mathrm{j}\omega_{\mathrm{osc}})\right| + F(\mathrm{j}3\omega_{\mathrm{in}})B(\mathrm{j}3\omega_{\mathrm{in}})}\right| \\ &\cdot\left(\left|\frac{F(\mathrm{j}\omega_{\mathrm{in}})}{2\left|F(\mathrm{j}\omega_{\mathrm{osc}})B(\mathrm{j}\omega_{\mathrm{osc}})\right| + F(\mathrm{j}\omega_{\mathrm{in}})B(\mathrm{j}\omega_{\mathrm{in}})}\right| \frac{\pi A_{\mathrm{in,s}}}{V_{\mathrm{DD}}}\right)^3 \\ &\cdot\left(1+\frac{9}{16}\left(\left|\frac{F(\mathrm{j}\omega_{\mathrm{in}})}{2\left|F(\mathrm{j}\omega_{\mathrm{osc}})B(\mathrm{j}\omega_{\mathrm{osc}})\right| + F(\mathrm{j}\omega_{\mathrm{in}})B(\mathrm{j}\omega_{\mathrm{in}})}\right| \frac{\pi A_{\mathrm{in,s}}}{V_{\mathrm{DD}}}\right)^2\right), \end{aligned} \tag{33}$$

$$\begin{aligned} \mathrm{HD}_3 &= \left|\frac{1}{F(\mathrm{j}3\omega_{\mathrm{in}})B(\mathrm{j}3\omega_{\mathrm{in}})}\right| \frac{A_{3\mathrm{in}}}{A_{\mathrm{out,s}}} \\ &= \frac{V_{\mathrm{DD}}}{12\pi A_{\mathrm{out,s}}}\cdot\left|\frac{F(\mathrm{j}\omega_{\mathrm{osc}})B(\mathrm{j}\omega_{\mathrm{osc}})}{2\left|F(\mathrm{j}\omega_{\mathrm{osc}})B(\mathrm{j}\omega_{\mathrm{osc}})\right| + F(\mathrm{j}3\omega_{\mathrm{in}})B(\mathrm{j}3\omega_{\mathrm{in}})}\right| \\ &\cdot\left(\left|\frac{F(\mathrm{j}\omega_{\mathrm{in}})}{2\left|F(\mathrm{j}\omega_{\mathrm{osc}})B(\mathrm{j}\omega_{\mathrm{osc}})\right| + F(\mathrm{j}\omega_{\mathrm{in}})B(\mathrm{j}\omega_{\mathrm{in}})}\right| \frac{\pi A_{\mathrm{in,s}}}{V_{\mathrm{DD}}}\right)^3 \\ &\cdot\left(1+\frac{9}{16}\left(\left|\frac{F(\mathrm{j}\omega_{\mathrm{in}})}{2\left|F(\mathrm{j}\omega_{\mathrm{osc}})B(\mathrm{j}\omega_{\mathrm{osc}})\right| + F(\mathrm{j}\omega_{\mathrm{in}})B(\mathrm{j}\omega_{\mathrm{in}})}\right| \frac{\pi A_{\mathrm{in,s}}}{V_{\mathrm{DD}}}\right)^2\right), \end{aligned} \tag{34}$$

where $F(\mathrm{j}3\omega_{\mathrm{in}})$ and $B(\mathrm{j}3\omega_{\mathrm{in}})$ are the values of $F(s)$ and $B(s)$ with $s=\mathrm{j}3\omega_{\mathrm{in}}$, respectively. The first two terms of $A_{3\omega_{\mathrm{in}}}$ in Eq. (19) are used to simplify the equation, since doing so does not introduce a large error according to Fig. 6.

Because $A_{\mathrm{out,s}}$ is proportional to $A_{\mathrm{in,s}}$ according to Eq. (31), the first product term of Eq. (34) is inversely proportional to $A_{\mathrm{in,s}}$. The second product term of Eq. (34) is not related to $A_{\mathrm{in,s}}$. The third product term of Eq. (34) is the third power of $A_{\mathrm{in,s}}$. The last product term of Eq. (34) increases with the increase of $A_{\mathrm{in,s}}$, and its slope also increases with the increase of $A_{\mathrm{in,s}}$. Thus, HD_3 increases with the increase of $A_{\mathrm{in,s}}$ at a slope larger than 12 dBc/oct, and its slope also increases with the increase of $A_{\mathrm{in,s}}$.

The relationship between HD_3 and ω_{in} is not obvious. However, due to the low-pass function of the filters $F(s)$ and $B(s)$, $|F(\mathrm{j}3\omega_{\mathrm{in}})B(\mathrm{j}3\omega_{\mathrm{in}})| > |F(\mathrm{j}3\omega_{\mathrm{in}})\cdot B(\mathrm{j}3\omega_{\mathrm{in}})| >> |F(\mathrm{j}\omega_{\mathrm{osc}})B(\mathrm{j}\omega_{\mathrm{osc}})|$ holds in high order SOPAs, and Eq. (34) can be simplified to Eq. (35). It can be observed from Eq. (35) that HD_3 decreases

with the decrease of ω_{in}, or decreases with the increase of ω_{osc}, which illustrates the distortion shaping character in high order SOPAs.

$$\mathrm{HD}_3 \approx \frac{V_{DD}}{12\pi A_{out,s}}\left|\frac{F(\mathrm{j}\omega_{osc})B(\mathrm{j}\omega_{osc})}{F(\mathrm{j}3\omega_{in})B(\mathrm{j}3\omega_{in})}\right| \cdot\left(\left|\frac{1}{B(\mathrm{j}\omega_{in})}\right|\frac{\pi A_{in,s}}{V_{DD}}\right)^3\left(1+\frac{9}{16}\left(\left|\frac{1}{B(\mathrm{j}\omega_{in})}\right|\frac{\pi A_{in,s}}{V_{DD}}\right)^2\right). \tag{35}$$

If the term $A_{3\omega_{in}}$ and the comparator's gain at $3\omega_{in}$ are replaced with the results in Piessens and Steyaert (2005), i.e., $V_{DD}/(16\pi)\cdot(A_{in}/A_{osc})^3$ and $V_{DD}/(\pi A_{osc})$, respectively, the same HD_3 calculation result as in Piessens and Steyaert (2005) can be obtained.

5 Simulation of the SOPA's third distortion

The block diagrams of the zeroth and the first order SOPA are shown in Fig. 8. In the zeroth order SOPA, there is no integrator in the forward path, which results in the transfer function $F(s)=1$ in Fig. 1. The transfer function of the feedback filter $B(s)=(\omega_{fil}/(s+\omega_{fil}))^3$ is chosen to satisfy the self-oscillation requirement (Piessens and Steyaert, 2005). In the first order SOPA, there is one integrator in the forward path. Its transfer function is $F(s)=k_1/s$, where k_1 is the unit gain angular frequency. k_1 can be arbitrary since the comparator detects only the polarity, but it is generally set to make the integrator's output less than the supply voltage. The transfer function of the feedback filter $B(s)=(\omega_{fil}/(s+\omega_{fil}))^2$ is chosen to satisfy the self-oscillation requirement.

The comparator's high- and low-level outputs $\pm V_{DD}=\pm 1$ V are chosen for both SOPAs. In the zeroth order SOPA, $\omega_{fil}=20\pi$ Mrad/s is chosen. According to

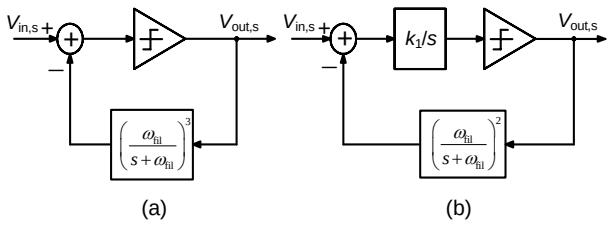

Fig. 8 Block diagram of the zeroth (a) and first order (b) self-oscillating power amplifier (SOPA)

the Barkhausen criterion and the transfer function of the filter, the limit cycle frequency is $\omega_{LC}=\tan(\pi/3)\omega_{fil}=20\sqrt{3}\pi$ Mrad/s, and the amplitude at the input of the comparator is $A_{LC}=(4V_{DD}/\pi)(\cos(\pi/3))^3=1/(2\pi)$ V.

In the first order SOPA, $\omega_{fil}=20\sqrt{3}\pi$ Mrad/s is chosen to have the same limit cycle frequency as the zeroth order SOPA. Choosing the unit gain angular frequency $k_1=10\sqrt{3}\pi$ Mrad/s and the limit cycle frequency $\omega_{LC}=\tan(\pi/4)\omega_{fil}=20\sqrt{3}\pi$ Mrad/s, the amplitude at the input of the comparator $A_{LC}=(4V_{DD}/\pi)(k_1/\omega_{LC})(\cos(\pi/4))^2=1/\pi$ V can be obtained.

Fig. 9 shows the simulation and calculation results of the output signal's amplitude $A_{out,s}$ relative to V_{DD} as a function of the input signal's amplitude $A_{in,s}/V_{DD}$. The input signal frequency is $\omega_{in}=2\pi$ Mrad/s. The simulation environment is MATLAB SIMULINK with an ODE45 solver. The amplitudes in the simulation results are derived from a 10^7-point DFT of the comparator's output with a simulation time of 10 μs and a sampling time of 1 ps. The window function of the DFT is Hanning. The simulation and calculation results agree reasonably well, especially in the first order SOPA. The assumption that the oscillation frequency ω_{osc} and amplitude A_{osc} are approximately equal to ω_{LC} and A_{LC}, respectively, introduces the errors in the calculation of the comparator's gain at ω_{in}, and $A_{out,s}$. The open-loop gain at frequency ω_{in} in the first order SOPA is smaller than that in the zeroth order SOPA, which makes the

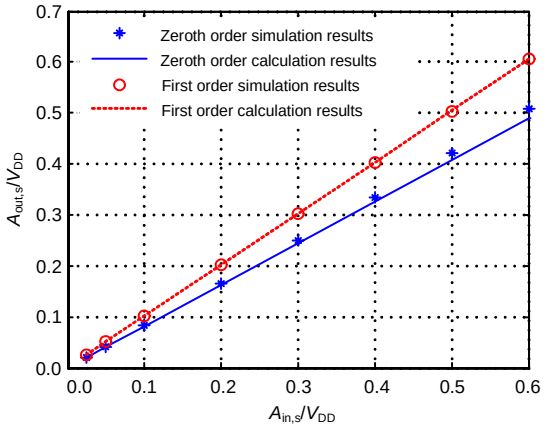

Fig. 9 Relationship between the output signal's amplitude $A_{out,s}/V_{DD}$ and the input signal's amplitude $A_{in,s}/V_{DD}$ with $\omega_{in}=2\pi$ Mrad/s

calculation errors in the first order SOPA smaller than those in the zeroth order SOPA. The open-loop gains at ω_{in} can be derived from Eq. (30), which are about 3.9 and 10.0 for the zeroth and the first order SOPA, respectively. The method to improve the loop gain according to Eq. (30) is out of the topic of this study.

Figs. 10 and 11 show the third harmonic distortion as a function of the input signal's amplitude $A_{in,s}/V_{DD}$ and frequency ω_{in}, respectively. The simulation environment is MATLAB SIMULINK with an ODE45 solver. The amplitudes in the simulation results are derived from a 10^7-point DFT of the comparator's output with a simulation time of 10 μs and a sampling time of 1 ps. The window function of the DFT is Hanning.

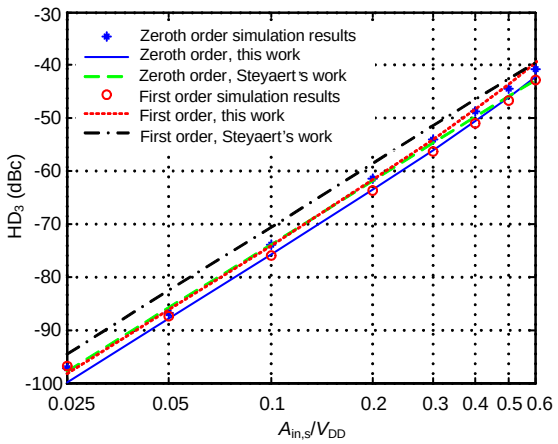

Fig. 10 Third harmonic distortion HD_3 as a function of the input signal amplitude $A_{in,s}$ with $\omega_{in}=2\pi$ Mrad/s

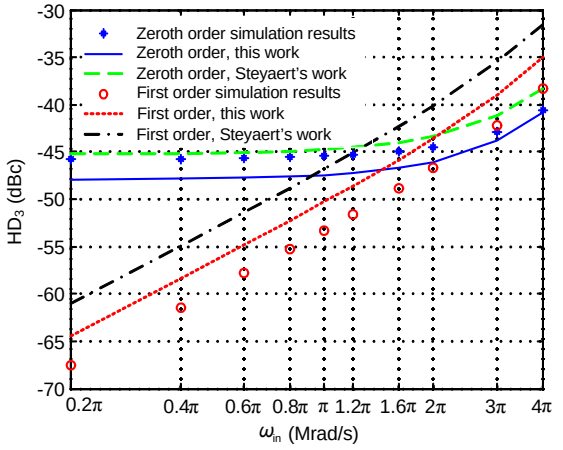

Fig. 11 Third harmonic distortion HD_3 as a function of the input signal frequency ω_{in} with $A_{in,s}/V_{DD}=0.5$

In Fig. 10, HD_3 of both the zeroth and the first order SOPA increases with the increase of $A_{in,s}$ with the slope slightly larger than 12 dB/oct, and the slope increases with the increase of $A_{in,s}$, which agrees with Eq. (34). Since a linear modulation is wanted, the input signal's amplitude cannot be too large. An HD_3 of −40 dBc is commonly not enough for many applications (Piessens and Steyaert, 2005). The larger $A_{in,s}/V_{DD}$ results in lower linearity, so $A_{in,s}/V_{DD}$ in Fig. 10 is up to 0.6. The HD_3 of the zeroth and the first order SOPA are close in this input frequency, but with a different input frequency the first order SOPA reveals its merit (Fig. 11).

In Fig. 11, with the increase of ω_{in}, HD_3 of the first order SOPA increases by approximately 6 dB/oct. In this range of ω_{in} in the first order SOPA, because $F(j3\omega_{in})$ is proportional to $1/\omega_{in}$, $B(j3\omega_{in})\approx1$ and $B(j\omega_{in})\approx1$; thus, it can be observed from Eq. (35) that HD_3 is proportional to $1/\omega_{in}$, which agrees reasonably well with the simulation results. In this range of ω_{in} in the zeroth order SOPA, $F(s)=1$ for all frequencies, $B(j\omega_{in})\approx1$, and when ω_{in} is small, $B(j3\omega_{in})$ decreases slowly with the increase of ω_{in}, but when ω_{in} is large, $B(j3\omega_{in})$ decreases more quickly. Thus, in the zeroth order SOPA, with the increase of ω_{in}, when ω_{in} is small, HD_3 increases slowly, and when ω_{in} is large, HD_3 increases more quickly, which agrees reasonably well with the simulation results. The distortion shaping character shows that higher order SOPA will have better linearity.

The calculation results in Piessens and Steyaert (2005) are also shown in Figs. 10 and 11 for comparison. The maximum error between the calculation and the simulation results for this work is about 3 dB, and it is about 6 dB for Steyaert's work. In the zeroth order SOPA, the Steyaert's work is slightly better than this work, while in the first order SOPA, this work is better. The two works are close, because their linearized models of the comparator are close, as described in Section 2, except for their different derivation processes.

The errors are introduced mainly by the assumption that the oscillation frequency ω_{osc} and the amplitude A_{osc} are approximately equal to the limit cycle frequency ω_{LC} and the amplitude A_{LC}, respectively (Section 4). Also, the approximations in the linearized model of the comparator and the approximations in the simplified equations introduce errors.

6 Conclusions

Calculating not only the fundamental, but also the third harmonic, components at the output of the comparator is a good method to linearize the comparator of the SOPA. The linearized model of the SOPA is created to describe the behavior, especially the relationships between the third harmonic distortion and the input signal's amplitude or frequency, which is useful for the designers to estimate the performance quickly. The models of the zeroth and the first order SOPA are compared to the behavioral simulation using MATLAB, and they match well. This work is slightly better than Steyaert's work with different derivation processes, and is useful for analyzing not only the third harmonic components, but also the other components.

References

Abramowitz, M., Stegun, I.A., 1972. Handbook of Mathematical Functions: with Formulas, Graphs, and Mathematical Tables (9th Ed.). Dover Publication, New York, p.255-294, 358-436. [doi:10.1119/1.15378]

Bailey, W.N., 1936. Some infinite integrals involving Bessel functions. *Proc. Lond. Math. Soc.*, **40**(1):37-48. [doi:10.1112/plms/s2-40.1.37]

Buyle, J., de Gezelle, V., Bakeroot, B., Doutreloigne, J., 2008. A High-Voltage Switching ADSL Line-Driver, with an n-Type Output Stage. Proc. 12th WSEAS Int. Conf. on Circuits, p.60-64.

Daniels, J., Dehaene, W., Steyaert, M., Wiesbauer, A., 2008. A 350-MHz Combined TDC-DTC with 61 ps Resolution for Asynchronous ΔΣ ADC Applications. IEEE Asian Solid-State Circuits Conf., p.365-368. [doi:10.1109/ASSCC.2008.4708803]

Daniels, J., Dehaene, W., Steyaert, M., Wiesbauer, A., 2010. A/D conversion using asynchronous delta-sigma modulation and time-to-digital conversion. *IEEE Trans. Circ. Syst. I: Reg. Papers*, **57**(9):2404-2412. [doi:10.1109/TCSI.2010.2043169]

de Gezelle, V., Doutreloigne, J., van Calster, A., 2005. A 765 mW high-voltage switching ADSL line driver. *Sol.-State Electron.*, **49**(12):1947-1950. [doi:10.1016/j.sse.2005.08.006]

de Gezelle, V., Buyle, J., Doutreloigne, J., 2008. Distortion Calculation of an Asynchronous Switching *x*DSL Line-Driver. IEEE Int. Symp. on Circuits and Systems, p.2386-2389. [doi:10.1109/ISCAS.2008.4541935]

Ekstrom, J.L., 1960. On infinite integrals containing products of Bessel functions. *SIAM Rev.*, **2**(1):23-26. [doi:10.1137/1002005]

Gelb, A., Velde, W.V., 1968. Multiple-Input Describing Functions and Nonlinear System Design. McGraw-Hill, New York, p.250-263.

Ouzounov, S., Roza, E., Hegt, J.A., van der Weide, G., van Roermund, A.H.M., 2006. Analysis and design of high-performance asynchronous sigma-delta modulators with a binary quantizer. *IEEE J. Sol.-State Circ.*, **41**(3):588-596. [doi:10.1109/JSSC.2005.864147]

Piessens, T., Steyaert, M., 2001. SOPA: a High Efficiency Line Driver in 0.35μm CMOS Using a Self Oscillating Power Amplifier. ISSCC Digest of Technical Papers, p.306-307. [doi:10.1109/ISSCC.2001.912650]

Piessens, T., Steyaert, M., 2003. Highly efficient *x*DSL line drivers in 0.35-μm CMOS using a self-oscillating power amplifier. *IEEE J. Sol.-State Circ.*, **38**(1):22-29. [doi:10.1109/JSSC.2002.806276]

Piessens, T., Steyaert, M., 2005. Behavioral analysis of self-oscillating class D line drivers. *IEEE Trans. Circ. Syst. I: Reg. Papers*, **52**(4):706-714. [doi:10.1109/TCSI.2005.844232]

Putzeys, B., 2005. Simple Self-oscillating Class D Amplifier with Full Output Filter Control. 118th AES Convention, No. 6453.

Roza, E., 1997. Analog-to-digital conversion via duty-cycle modulation. *IEEE Trans. Circ. Syst. II: Anal. Dig. Signal Process.*, **44**(11):907-914. [doi:10.1109/82.644044]

Serneels, B., Steyaert, M., Dehaene, W., 2007. A 237mW aDSL2+ CO Line Driver in Standard 1.2 V 0.13μm CMOS. ISSCC Digest of Technical Papers, p.524-619. [doi:10.1109/ISSCC.2007.373525]

van der Hulst, P., Veltman, A., Groenenberg, R., 2002. An Asynchronous Switching High-End Power Amplifier. 112th AES Convention, No. 5503.